

background (3). The visual scoring scheme has been confirmed by histology as described [S. Parangi *et al.*, *Cancer Res.* **55**, 66071 (1995)].

14. Microdissected tumors and pancreases were immersion-fixed in 4% paraformaldehyde and embedded in paraffin. Apoptotic index and vessel density were assessed by combined TUNEL [P. Naik *et al.*, *Genes Dev.* **10**, 2105 (1996)] and CD31 staining. Apoptotic labeling was followed by CD31 staining with a 1:100 dilution of a rat anti-mouse CD31 monoclonal antibody (Pharmingen). Reaction products were visualized with an ABC

kit, using as chromophores 3,3-diaminobenzidine (for TUNEL-positive cells) and alkaline phosphatase substrate (for CD31 staining). Proliferating cells were detected with a mouse antibody against human proliferation-associated nuclear antigen (Biogenex). Ten to 20 fields of the respective sections were scored under oil immersion light microscopy.

15. G. Bergers, K. Javaherian, K.-M. Lo, J. Folkman, D. Hanahan, data not shown.  
16. S. N. Grant, I. Seidman, D. Hanahan, *Cancer Res.* **51**, 4917 (1991).

17. We thank British Biotech Pharmaceuticals, Oxford, UK, for BB-94 and Takeda-Abbott Pharmaceuticals for AGM1470; S. Gillies of Letigan Pharmaceuticals for advice and support of the production of Fc-endostatin and Fc-angiostatin; E. Soliven for excellent technical assistance; A. McMillan for statistical analysis; and R. Weinberg, R. Klausner, J. M. Bishop, J. D. Watson, S. Parangi, J. Hager, E. Bergsland, and H. Ee for comments and critical reading of the manuscript. Supported by grants from the National Cancer Institute.

5 January 1999; accepted 30 March 1999

## Unexpected Modes of PDZ Domain Scaffolding Revealed by Structure of nNOS-Syntrophin Complex

Brian J. Hillier,<sup>1</sup> Karen S. Christopherson,<sup>2</sup> Kenneth E. Prehoda,<sup>1</sup> David S. Brecht,<sup>2</sup> Wendell A. Lim<sup>1\*</sup>

The PDZ protein interaction domain of neuronal nitric oxide synthase (nNOS) can heterodimerize with the PDZ domains of postsynaptic density protein 95 and syntrophin through interactions that are not mediated by recognition of a typical carboxyl-terminal motif. The nNOS-syntrophin PDZ complex structure revealed that the domains interact in an unusual linear head-to-tail arrangement. The nNOS PDZ domain has two opposite interaction surfaces—one face has the canonical peptide binding groove, whereas the other has a  $\beta$ -hairpin "finger." This nNOS  $\beta$  finger docks in the syntrophin peptide binding groove, mimicking a peptide ligand, except that a sharp  $\beta$  turn replaces the normally required carboxyl terminus. This structure explains how PDZ domains can participate in diverse interaction modes to assemble protein networks.

PDZ protein interaction domains (1) play a central role in organizing diverse signaling pathways (2–7). The scaffolding protein InaD (inactivation no after potential), which comprises five PDZ domains, tethers multiple proteins of the *Drosophila* phototransduction cascade (6). The postsynaptic density protein PSD-95, which has three PDZ domains, clusters and localizes *N*-methyl-D-aspartic acid (NMDA)-type glutamate receptors at synapses (2). By organizing such protein networks, PDZ scaffolding proteins increase the efficiency and specificity of signal transduction.

Most known PDZ-mediated interactions occur through recognition of short COOH-terminal peptide motifs (2). Peptide interaction screens indicate that the terminal carboxylate of these ligands is required for binding (8). This canonical mode of PDZ recognition is well characterized: structures of PDZ-peptide complexes reveal that recognition is achieved through an extended binding groove

that terminates in a conserved carboxylate binding loop (9, 10).

Nonetheless, an increasing number of PDZ-mediated interactions occur through modes that are not dependent on recognition of a COOH-terminal motif. A well-characterized example is the PDZ domain of neuronal nitric oxide synthase (nNOS), the neuron- and muscle-specific isoform of the enzyme that produces the second

messenger nitric oxide (NO). The PDZ domain of nNOS specifically heterodimerizes with PDZ domains from PSD-95 and syntrophin in neurons and muscle cells, respectively (5). These interactions allow the integration of nNOS into specific signaling pathways. Association with PSD-95 in neurons is thought to couple NO production to NMDA receptor activation (11). Association with syntrophin in muscle cells localizes nNOS to the dystrophin complex (12), coupling NO production to muscle contraction. The resulting NO exerts a protective effect by increasing blood flow to match the heightened metabolic load of contracting muscle. Loss of this response in Duchenne muscular dystrophy may contribute to muscle degeneration (13).

These PDZ-PDZ interactions are distinct from canonical PDZ-peptide interactions in that they do not involve recognition of a COOH-terminal sequence on either partner protein. Moreover, the full tertiary structures of both PDZ partners are required, including 30 amino acids in nNOS that extend beyond the canonical PDZ region (5). These interactions are representative of an alternative class of PDZ domain interactions: the recognition of internal motifs. Such internal interactions have also been reported for PDZ domains from the scaffolding proteins GRIP and InaD (7, 14).

We determined the crystal structures of the nNOS PDZ domain alone and in complex with the syntrophin PDZ domain to 1.25 and 1.9 Å resolution, respectively (15) (Table 1).

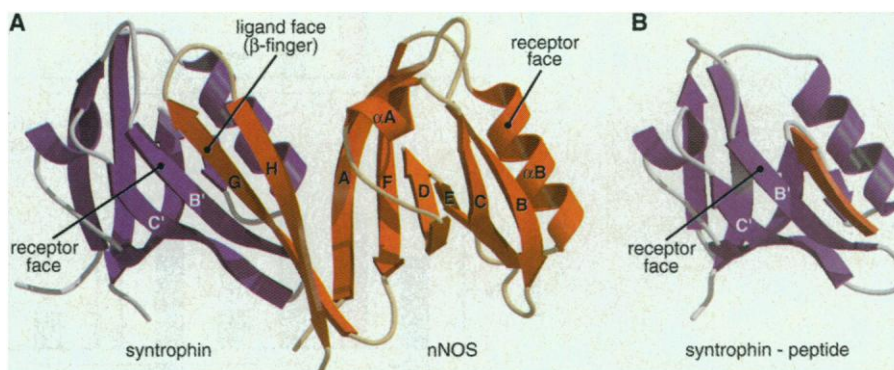


**Fig. 1.** Linear head-to-tail heterodimer of nNOS-syntrophin PDZ domains. (A) The nNOS PDZ domain (orange) has a polarized structure with distinct receptor (peptide binding groove) and ligand ( $\beta$ -finger) faces. The nNOS ligand face docks against the syntrophin PDZ domain (purple) peptide binding groove. (B) Structure of the syntrophin PDZ domain (purple) in complex with a COOH-terminal peptide (orange) (10). The figure was generated with the program MOLSCRIPT (25).

<sup>1</sup>Department of Cellular and Molecular Pharmacology and Department of Biochemistry and Biophysics, <sup>2</sup>Department of Physiology, University of California, San Francisco, San Francisco, CA 94143, USA.

\*To whom correspondence should be addressed. E-mail: wlim@itsa.ucsf.edu

REPORTS

Table 1. Summary of crystallographic analysis. Dashes indicate entries that are meaningless for native data sets alone.

Crystal	Resolution limit (Å)	Reflections (measured/unique)	Completeness	$R_{sym}$ § (highest bin)	Phasing double bar power	$R_{cullis}$ ¶ acentric		
Complex*								
Native‡	1.9	123,446/15,442	90.6	11.2 (8.8)	—	—		
S55C I (HgCl <sub>2</sub> )	2.6	29,484/4,570	67.2	4.4 (8.5)	2.6	0.64		
S55C II (HgCl <sub>2</sub> )	2.0	47,260/11,721	81.1	5.8 (13.4)	1.8	0.76		
A60C (MeHgCl)	2.7	20,425/5,497	90.0	18.2 (68.4)	1.4	0.86		
nNOS†								
Native‡	1.25	131,703/33,078	98.9	3.8 (29.0)	—	—		
S55C (HgCl <sub>2</sub> )	2.2	30,112/5,673	88.4	7.5 (23.3)	2.4	0.64		
A60C (MeHgCl)	1.7	48,045/12,811	95.5	3.9 (16.8)	1.8	0.75		
	Resolution (Å)	No. of reflections	Completeness	R factor#	Free R factor**	Bond length (rmsd)††	Bond angle (rmsd)††	Average B
Complex	50–1.9	15,162	89.3	20.8	25.9	0.005	1.34	19.3
nNOS	50–1.25	31,989	95.8	23.9	25.5	0.004	1.39	15.7

\*Complex: space group  $P2_12_12_1$ ;  $a = 31.58$ ,  $b = 34.31$ ,  $c = 187.83$ ; one complex per asymmetric unit. †nNOS: space group  $P2_12_12_1$ ;  $a = 35.18$ ,  $b = 38.99$ ,  $c = 85.60$ ; one molecule per asymmetric unit. ‡Merged high- and low-resolution data sets. § $R_{sym} = 100 \times \sum_i |I_i - \langle I \rangle| / \sum_i I_i$ . ||Phasing power =  $\langle F_H \rangle / E_{rms}$ . ¶ $R_{cullis} = \sum |F_{deriv} - F_{nat}| - |F_{Hcalc}| / \sum |F_{deriv} - F_{nat}|$ . #R factor =  $\sum |F_{obs} - F_{calc}| / \sum F_{obs}$ . \*\*10% of data was used for calculation of free R factor. ††rmsd, root mean square deviation.

These structures reveal the mechanism of PDZ heterodimerization and, more generally, of internal sequence recognition. The nNOS and syntrophin PDZ domains associate in a linear head-to-tail fashion that lacks the two-fold rotational symmetry normally observed in dimer structures (Fig. 1). Linear association occurs because the nNOS PDZ domain has an unusual polarized structure with two distinct faces: a receptor face, comprising the canonical PDZ domain with its peptide binding groove (residues 1 to 100), and a ligand face, comprising a  $\beta$ -hairpin “finger” (resi-

dues 100 to 130). This  $\beta$  finger acts as a PDZ ligand, docking into the peptide binding groove of the syntrophin PDZ domain. The two-stranded nNOS  $\beta$  finger augments an antiparallel  $\beta$  sheet in syntrophin, forming a composite four-stranded sheet (16). In the complex, the peptide binding groove of the nNOS PDZ domain remains accessible to interact with additional proteins.

The first strand of the nNOS  $\beta$  finger (referred to as the pseudo-peptide motif) mimics a canonical COOH-terminal peptide ligand in its sequence-specific interactions with the syntro-

phin PDZ domain (Fig. 2) (17). However, the normally required terminal carboxylate of a peptide ligand is replaced by the sharp  $\beta$  turn at the tip of the nNOS  $\beta$  finger.

The existence of this complex demonstrates that a terminal carboxylate group is not an absolute requirement for PDZ recognition. In canonical PDZ complexes, the ligand terminal carboxylate is cradled in the GLGF (18), or carboxylate binding, loop found at the end of the binding groove (19). Because the nNOS  $\beta$  finger lacks a carboxylate, yet still serves as a specific ligand, we propose that the GLGF loop

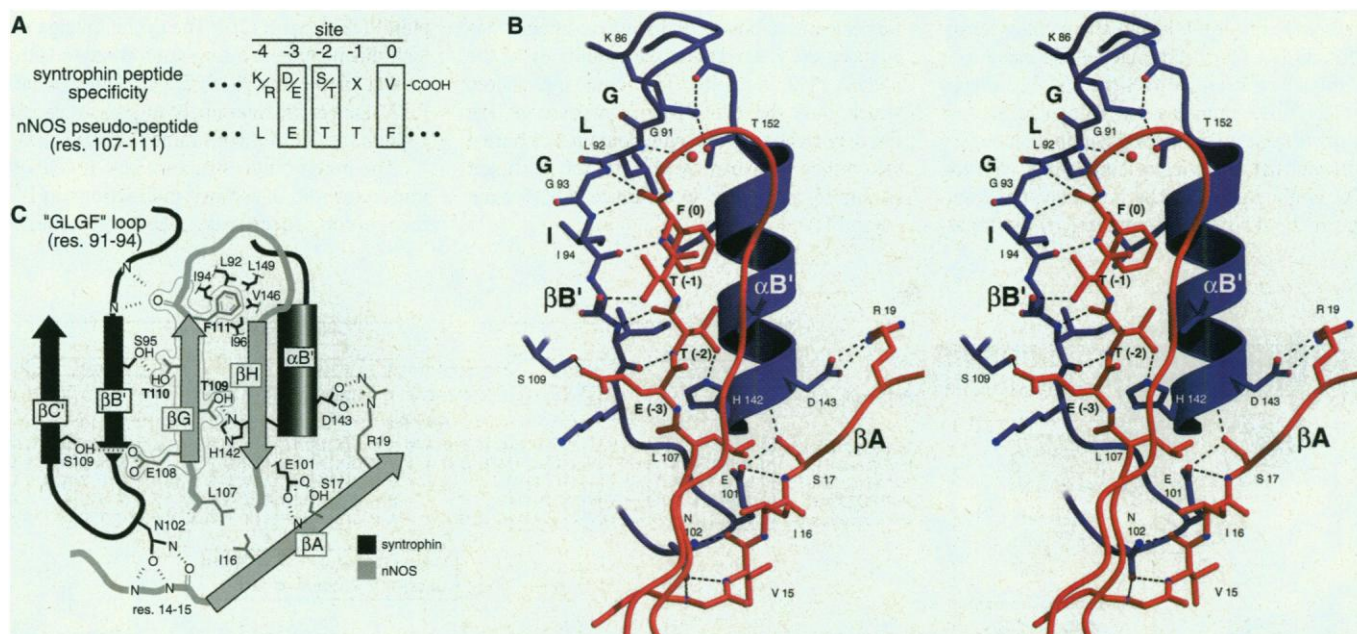
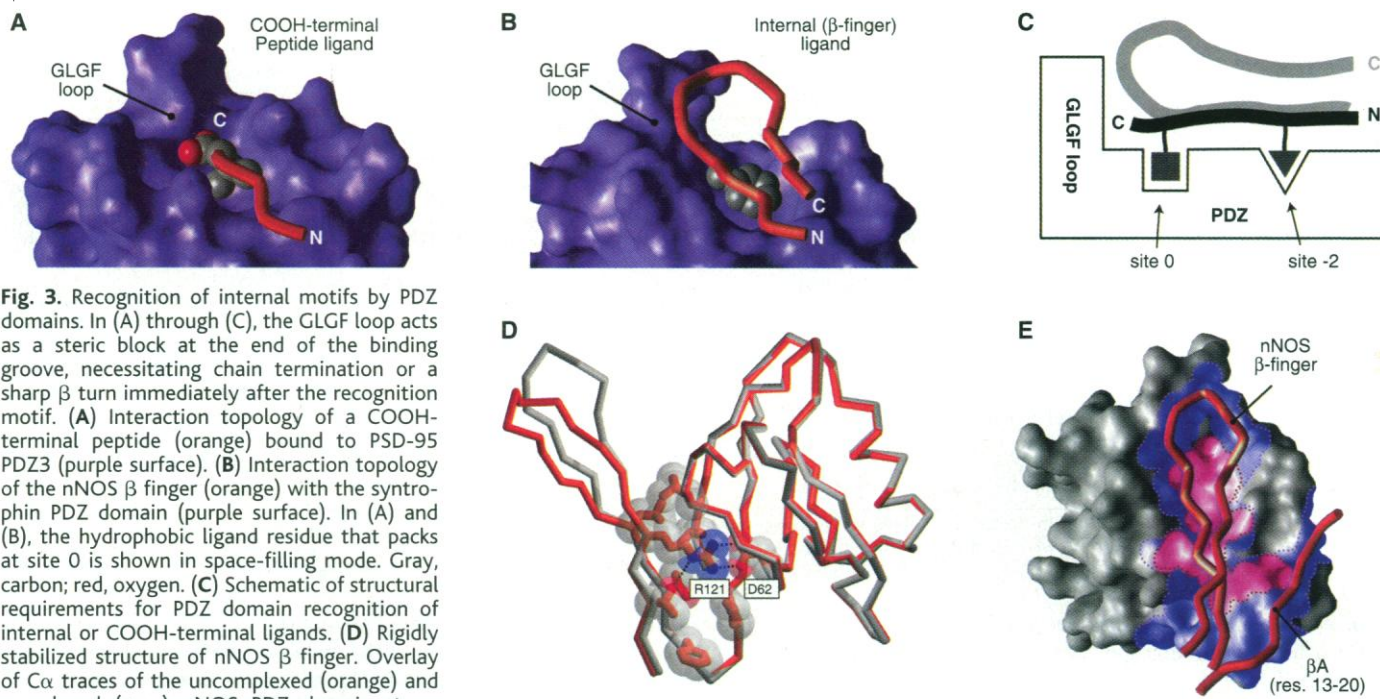


Fig. 2. Presentation of the nNOS  $\beta$  finger as an internal sequence motif that mimics a COOH-terminal PDZ peptide ligand. (A) Sequence comparison of syntrophin PDZ domain preferred COOH-terminal peptide ligands (10) with the nNOS pseudo-peptide (18). Binding site nomenclature is from (9). (B) Stereo depiction of the nNOS  $\beta$  finger (orange) bound at the syntrophin (purple) binding groove. nNOS pseudo-peptide residues are indicated by the binding pocket number (in parentheses). All

other numbers refer to the actual residue number. The GLGF/carboxylate binding loop (19) is highlighted. Hydrogen bonds are shown as dashed lines, and an ordered water molecule is shown as a red sphere. For clarity, nNOS strand H is shown as a  $C\alpha$  trace, and its backbone hydrogen bonds have been omitted. The image was generated with the program MOL-SCRIPT (25). (C) Schematic depiction of heterodimer interface interactions. The nNOS pseudo-peptide segment is outlined.

REPORTS



**Fig. 3.** Recognition of internal motifs by PDZ domains. In (A) through (C), the GLGF loop acts as a steric block at the end of the binding groove, necessitating chain termination or a sharp  $\beta$  turn immediately after the recognition motif. (A) Interaction topology of a COOH-terminal peptide (orange) bound to PSD-95 PDZ3 (purple surface). (B) Interaction topology of the nNOS  $\beta$  finger (orange) with the syntrophin PDZ domain (purple surface). In (A) and (B), the hydrophobic ligand residue that packs at site 0 is shown in space-filling mode. Gray, carbon; red, oxygen. (C) Schematic of structural requirements for PDZ domain recognition of internal or COOH-terminal ligands. (D) Rigidly stabilized structure of nNOS  $\beta$  finger. Overlay of  $\alpha$  traces of the uncomplexed (orange) and complexed (grey) nNOS PDZ domain structures, highlighting residues that stabilize the nNOS  $\beta$ -finger conformation. The main interaction is a salt bridge between Arg<sup>121</sup> and Asp<sup>62</sup>, which is buried by the surrounding hydrophobic residues Ile<sup>16</sup>, Leu<sup>57</sup>, Pro<sup>100</sup>, Phe<sup>103</sup>, Thr<sup>105</sup>, Leu<sup>107</sup>, and Thr<sup>123</sup>. (E) Increased contact area in the PDZ heterodimer through tertiary interactions. Solvent excluded

footprint of the nNOS PDZ domain ( $\alpha$  trace shown in orange) bound to the syntrophin PDZ domain (purple surface,  $\sim 800 \text{ \AA}^2$ ), compared to the footprint of a peptide ligand (pink surface,  $\sim 400 \text{ \AA}^2$ ). Images were generated with the programs MOLSCRIPT (25) and WebLab Viewer Lite (26).

serves another function aside from carboxylate recognition: acting as a steric block to prevent binding of peptides that extend beyond the recognition sequence (Fig. 3, A through C). The restriction imposed by such a block can be overcome only if the ligand chain either terminates, as do COOH-terminal peptide ligands, or folds back on itself, as does the nNOS  $\beta$  finger.

Thus PDZ domains can recognize internal motifs if these are presented within a secondary structure that is sterically compatible with the PDZ binding groove. The importance of a stable structural context is supported by the appar-

ent conformational rigidity of the nNOS  $\beta$  finger. Despite extending far from the main body of the domain, the  $\beta$  finger adopts essentially the same structure in the crystals of the nNOS PDZ domain alone (Fig. 3D). This rigid conformation is stabilized by extensive interactions between the  $\beta$  finger and the main body of the nNOS PDZ domain. The core interaction, which pins the COOH-terminal base of the finger back against the main domain, is a buried salt bridge between Arg<sup>121</sup> in the  $\beta$  finger (strand H) and Asp<sup>62</sup> in the main PDZ domain (strand D).

Stabilization of the nNOS  $\beta$ -finger structure appears to be critical because the entire folded nNOS PDZ domain is required for interaction (5). Moreover, a cyclic peptide that bears an internal recognition motif can bind the syntrophin PDZ domain (20). The cyclic linkage may lock this peptide in a turn conformation similar to that of the nNOS  $\beta$  finger. Other internal PDZ ligands are also likely to present pseudopeptide motifs in a constrained context (21).

The heterodimer structure also reveals the important role of tertiary interactions in PDZ recognition specificity. Many residues in

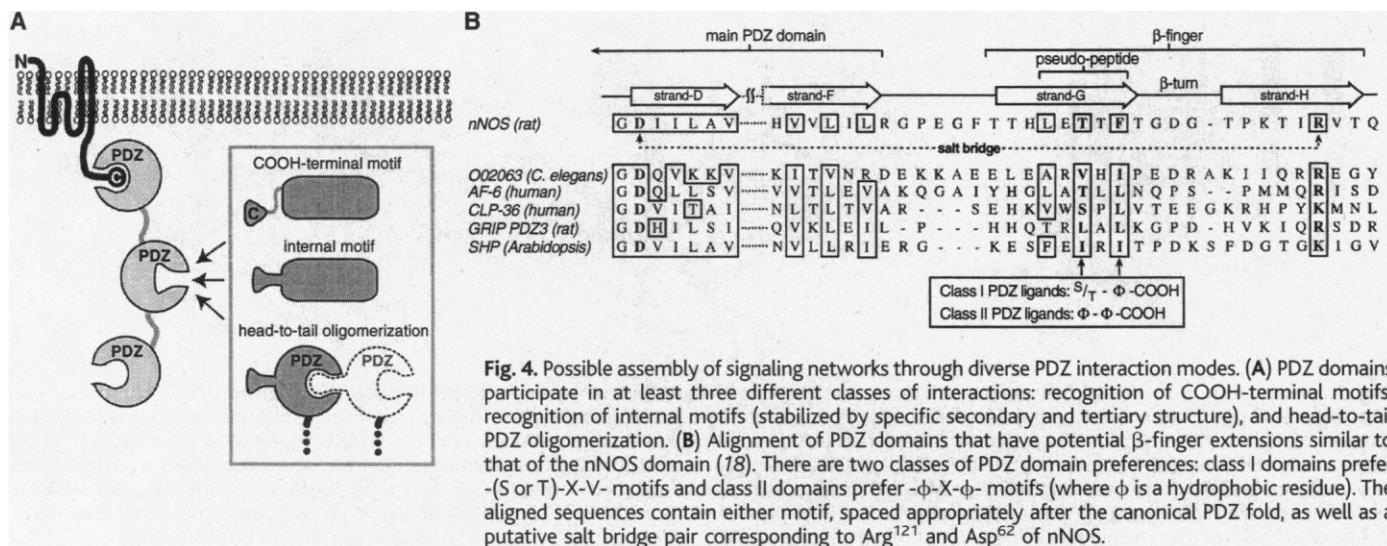


**Fig. 4.** Possible assembly of signaling networks through diverse PDZ interaction modes. (A) PDZ domains participate in at least three different classes of interactions: recognition of COOH-terminal motifs, recognition of internal motifs (stabilized by specific secondary and tertiary structure), and head-to-tail PDZ oligomerization. (B) Alignment of PDZ domains that have potential  $\beta$ -finger extensions similar to that of the nNOS domain (18). There are two classes of PDZ domain preferences: class I domains prefer -(S or T)-X-V- motifs and class II domains prefer - $\Phi$ -X- $\Phi$ - motifs (where  $\Phi$  is a hydrophobic residue). The aligned sequences contain either motif, spaced appropriately after the canonical PDZ fold, as well as a putative salt bridge pair corresponding to Arg<sup>121</sup> and Asp<sup>62</sup> of nNOS.

nNOS and syntrophin that participate in heterodimerization are distant in sequence from the primary pseudo-peptide contacts. As a result, heterodimerization buries twice the surface area on the syntrophin PDZ domain as compared to binding of a peptide ligand (Fig. 3E). Most of the additional tertiary contacts come from the most NH<sub>2</sub>-terminal strand of the nNOS PDZ domain (strand A), which in the complex packs against the syntrophin  $\alpha$  helix. Residues that participate in this ensemble of primary and tertiary interactions (Ser<sup>95</sup>, Asn<sup>102</sup>, Ser<sup>109</sup>, His<sup>142</sup>, and Asp<sup>143</sup>) are uniquely conserved in the syntrophin and PSD-95 (second domain) PDZ domains, perhaps explaining why only these two domains heterodimerize with nNOS (22). Analogous tertiary interactions may also enhance the specificity of COOH-terminal peptide-mediated PDZ interactions (23).

The linear head-to-tail arrangement observed in the syntrophin-nNOS complex may allow PDZ proteins to achieve more than subcellular localization (Fig. 4A). Correct targeting of nNOS could be achieved by simply appending an appropriate COOH-terminal sequence. The bifunctional (that is, receptor and ligand) nNOS PDZ domain, however, in addition to localizing its cargo protein (the catalytic portion of NOS), adds on a new receptor site with altered specificity that can recruit additional proteins (24). Bifunctional PDZ domains could also oligomerize to yield heteropolymer filaments. Indeed, the polarized structure of the nNOS PDZ domain is typical of cytoskeletal filament monomers or viral capsid proteins, both of which form higher order repeating assemblies. Finally, these types of domains could mediate branching interactions between proteins with multiple PDZ domains. A search of known PDZ sequences revealed several that may have a nNOS type of  $\beta$  finger immediately COOH-terminal to the canonical PDZ domain (Fig. 4B).

These structures reveal that PDZ domains can interact in multiple ways—recognizing COOH-terminal or constrained internal motifs and forming head-to-tail oligomers. The ability of PDZ domains to participate in these diverse interactions and their potential to form higher order assemblies may explain why these modules so often mediate scaffolding of sophisticated signaling networks at synapses and other critical membrane sites.

References and Notes

1. The name PDZ is derived from the first three proteins in which these domains were identified: PSD-95, the *Drosophila* septate junction protein Discs-Large (Dlg), and the epithelial tight junction protein ZO-1.
2. E. Kim *et al.*, *Nature* **378**, 85 (1995); H. C. Kornau *et al.*, *Science* **269**, 1737 (1995); T. Sato *et al.*, *ibid.* **268**, 411 (1995).
3. J. S. Simsk *et al.*, *Cell* **85**, 195 (1996); H. Dong *et al.*, *Nature* **386**, 279 (1997).
4. A. S. Fanning and J. M. Anderson, *Curr. Biol.* **6**, 1385 (1996); S. K. Kim, *Curr. Opin. Cell Biol.* **9**, 853 (1997);

- R. Ranganathan and E. M. Ross, *Curr. Biol.* **7**, R770 (1997); S. E. Craven and D. S. Brett, *Cell* **93**, 495 (1998).
5. J. E. Brenman *et al.*, *Cell* **84**, 757 (1996); J. E. Brenman *et al.*, *J. Neurosci.* **16**, 7407 (1996).
6. S. Tsunoda *et al.*, *Nature* **388**, 243 (1997); J. Cheveschich, A. J. Kreuz, C. Montell, *Neuron* **18**, 95 (1997).
7. X. Z. Xu *et al.*, *J. Cell Biol.* **142**, 545 (1998).
8. Z. Songyang *et al.*, *Science* **275**, 73 (1997).
9. D. A. Doyle *et al.*, *Cell* **85**, 1067 (1996); J. H. Cabral *et al.*, *Nature* **382**, 649 (1996); D. L. Daniels *et al.*, *Nature Struct. Biol.* **5**, 317 (1998).
10. J. Schultz *et al.*, *Nature Struct. Biol.* **5**, 19 (1998).
11. Disrupting the nNOS/PSD-95 interaction is a major pharmacological goal, because overstimulation of NMDA receptors during cerebral ischemia produces neurotoxic amounts of NO that cause brain injury [T. M. Dawson, V. L. Dawson, S. H. Snyder, *Ann. Neurol.* **32**, 297 (1992); Z. Huang *et al.*, *Science* **265**, 1883 (1994)].
12. J. E. Brenman *et al.*, *Cell* **82**, 743 (1995).
13. G. D. Thomas *et al.*, *Proc. Natl. Acad. Sci. U.S.A.* **95**, 15090 (1998); K. S. Lau *et al.*, *FEBS Lett.* **431**, 71 (1998).
14. E. Cuppen *et al.*, *Mol. Biol. Cell* **9**, 671 (1998); R. van Huizen *et al.*, *EMBO J.* **17**, 2285 (1998).
15. Proteins were expressed in *E. coli* strain BL21(DE3) as fusion proteins with a cleavable hexahistidine (His<sub>6</sub>) tag at the NH<sub>2</sub>-terminus using a pET19b derived vector (Novagen). Cells were lysed by sonication. After centrifugation, the supernatant was loaded onto a column of Nickel-NTA resin (Qiagen). After washing, the proteins were eluted with 0.5 M imidazole. The His<sub>6</sub> tag was removed by cleavage with TEV (tobacco etch viral) protease for 2 hours at room temperature, after which the reaction mixture was passed over a second Nickel-NTA column. Proteins were loaded onto a SourceS (Pharmacia) column and eluted with a gradient of NaCl (0 to 1000 mM), dialyzed into 20 mM Hepes (pH 7), concentrated to 15 mg/ml, flash-frozen, and stored at -80°C. The fragments used for crystallization were rat nNOS amino acids 1 through 130 and mouse  $\alpha$ -1 syntrophin amino acids 77 through 171, both containing a vector-derived sequence Gly-Ser at the NH<sub>2</sub>-terminus. The complex [from a mixture of syntrophin PDZ domain (7.3 mg/ml) and nNOS PDZ domain (5.5 mg/ml)] was crystallized by vapor diffusion against 100 mM tris (pH 8.5), 25% PEG4000, and 0.2 M sodium acetate at room temperature. nNOS PDZ domain alone (10 mg/ml) was crystallized against 100 mM tris (pH 8.5) and 15% PEG4000. Crystals were soaked in a cryoprotectant of crystallization buffer with 15% glucose for 15 min before flash freezing. Native and derivative data sets (Table 1) were collected with a rotating anode x-ray source at the Advanced Light Source beamline 5.0.2 (Lawrence Berkeley Laboratories) and the Stanford Synchrotron Radiation Laboratory. Data were processed with the programs DENZO/SCALEPACK [Z. Otwinoski and W. Minor, *Methods Enzymol.* **276**, 307 (1997)]. We were unable to solve either structure by molecular replacement, and instead generated site-specific cysteine mutations [Ser<sup>55</sup>  $\rightarrow$  Cys<sup>55</sup> (S55C) and Ala<sup>60</sup>  $\rightarrow$  Cys<sup>60</sup> (A60C)] to obtain mercury derivatives. Initial mercury atom positions were found with the use of the program SOLVE [T. C. Terwilliger and J. Berendzen, *Acta Crystallogr.* **D52**, 749 (1996)], and positions were refined with the program SHARP [E. de la Fortelle and G. Bricogne, *Methods Enzymol.* **276**, 472 (1997)]. The resulting electron density map was subjected to solvent flattening with the program SOLMON [CCP4: A Suite of Programs for Protein Crystallography (SERC Daresbury Laboratory, Warrington, UK, 1979)]. Map interpretation and model building were done with the program O [T. A. Jones *et al.*, *Acta Crystallogr.* **D52**, 30 (1996)]. The structures were subjected to cycles of positional and restrained individual B-factor refinement and to a bulk solvent correction with the program CNS [A. T. Brünger *et al.*, *ibid.* **D54**, 905 (1998)].
16. This mechanism of association, referred to as  $\beta$ -strand invasion or  $\beta$ -strand augmentation [S. C. Harrison, *Cell* **86**, 341 (1996)], is commonly observed in the interactions of viral capsid assembly proteins.
17. There are two minor ways in which the nNOS pseudo-peptide differs from a COOH-peptide ligand. First, the

terminal residue (site 0) in the nNOS pseudo-peptide is a phenylalanine instead of valine. The larger phenylalanine may be required to fill the site 0 hydrophobic pocket because, at this point, the peptide chain is displaced somewhat further away from the syntrophin surface than is a peptide ligand. Second, the nNOS pseudo-peptide has a leucine at site -4, in place of the usual basic residue. In the syntrophin PDZ-peptide complex (10), the basic residue at this position is recognized through a salt bridge interaction with Asp<sup>143</sup> of syntrophin. In the nNOS-syntrophin complex, Asp<sup>143</sup> interacts with nNOS residue Arg<sup>19</sup> in strand A of the nNOS PDZ domain (Fig. 2, B and C). Thus the site -4 interaction in a peptide complex is replaced by a tertiary interaction in the heterodimer complex.

18. Single-letter abbreviations for the amino acid residues are as follows: A, Ala; C, Cys; D, Asp; E, Glu; F, Phe; G, Gly; H, His; I, Ile; K, Lys; L, Leu; M, Met; N, Asn; P, Pro; Q, Gln; R, Arg; S, Ser; T, Thr; V, Val; W, Trp; and Y, Tyr.
19. This loop includes the well-conserved GLGF motif, although this exact sequence is not absolutely maintained in all PDZ domains (it is GLGI in syntrophin). In COOH-peptide complexes (9, 10), the terminal carboxylate of the ligand is bound through four hydrogen bonds: three with the amide nitrogens of the GLGF loop and one with a well-ordered water molecule. This water molecule is held in position by a conserved Arg or Lys residue that occurs just NH<sub>2</sub>-terminal to the GLGF loop. The nNOS  $\beta$  finger can only participate in two of these four hydrogen bonds. Given that both ligand types are similar in affinity (B. Hillier, unpublished data), either the energetic contribution of these hydrogen bonds is small or the tertiary interactions observed in the heterodimer compensate for their loss. In PDZ-peptide complexes, no direct charge-charge interactions are made with the terminal carboxylate (the interaction with the conserved basic residue is mediated by a water molecule). This property, which sets the PDZ domain apart from most examples of carboxylate recognition proteins, may explain why a molecule like the nNOS  $\beta$  finger, which lacks a formal negative charge at its tip, still functions as a ligand.
20. S. H. Gee *et al.*, *J. Biol. Chem.* **273**, 21980 (1998).
21. A PDZ domain from the protein tyrosine phosphatase BL binds an internal motif in the RIL (reversion-induced LIM gene) protein, and a PDZ domain from InaD binds an internal motif from the protein phospholipase C- $\beta$  (PLC- $\beta$ ) (14). The RIL protein contains the sequence GLNLKQRGY, and PLC- $\beta$  contains the sequence QIGVVKQGR. Both are consistent with class II PDZ motifs, followed by turn-preferring residues. For turn preferences, see B. L. Sibanda and J. M. Thornton, *Methods Enzymol.* **202**, 59 (1991).
22. The nNOS PDZ domain can also interact with the second PDZ domain from PSD-93. However, PSD-93 is an isoform of PSD-95 that is nearly identical in sequence (5).
23. M. Niethammer *et al.*, *Neuron* **20**, 693 (1998).
24. J. Schepens *et al.*, *FEBS Lett.* **409**, 53 (1997); N. L. Stricker *et al.*, *Nature Biotechnol.* **15**, 336 (1997).
25. P. J. Kraulis, *J. Appl. Crystallogr.* **24**, 946 (1991).
26. WebLab ViewerLite 3.1 for Power Macintosh, Molecular Simulations Inc.
27. Supported by grants from NIH (W.A.L. and D.S.B.); by awards to W.A.L. from the Howard Hughes Medical Institute Research Resources Program, the Burroughs Wellcome Fund, the Searle Scholars Program, and the Packard Foundation; and by awards to D.S.B. from the National Association for Research on Schizophrenia and Depression and the EJLB and Culpeper Foundations. K.E.P. is a Cancer Research Institute postdoctoral fellow. We thank T. Earnest and the staff of the Macromolecular Crystallography Facility at the Advanced Light Source (Department of Energy, Lawrence Livermore National Laboratory), P. Foster, T. Gonzalez, E. Ruttenberg, K. Thorn, and members of the University of California San Francisco Macromolecular Structure Group for assistance; and H. Bourne, D. Julius, R. Nicoll, J. Weissman, and members of the Lim laboratory for comments. Coordinates have been deposited in the Protein Data Bank (ID codes 1QAU and 1QAV).

4 February 1999; accepted 1 April 1999